13TH CANADIAN MASONRY SYMPOSIUM
HALIFAX, CANADA
JUNE 4TH – JUNE 7TH 2017

BEHAVIOUR OF STACK PATTERN MASONRY BEAMS

Zohrehheydariha, Jamshid[1]; Das, Sreekanta[2] and Banting, Bennett[3]

ABSTRACT
Clause 11 of the Canadian standard, CSA S304 currently does not allow stack pattern masonry beams to be designed and built with the provisions laid within. However, many architects opt for the stack pattern masonry look for aesthetic purposes not realizing the structural limitations it has. As a result, designers are placed in precarious position trying to reconcile the selected bonding pattern with the requirements and limitations of the CSA S304. Since the head joints in stack pattern masonry line up vertically, it is believed that this construction is weaker than the traditional running bond construction. However, since masonry beams must be fully-grouted the effects of aligned head joints can be mitigated by increasing the grouted area of the units and the horizontal grout continuity in the beam. This study was completed to determine the structural behaviour of stack pattern masonry beams and prisms utilizing units with reduced webs to accommodate horizontal grout continuity. A total of eight full-scale masonry beams and twenty prisms were tested in the structural engineering laboratory of University of Windsor detailed with both running bond and stack pattern coursing. This study found that although the cracks at the head joints of the stack pattern beam specimens initiated at lower loads, the ultimate strength, stiffness and deflection for both bonding patterns were similar. This paper discusses the test specimens and test results obtained from this study and demonstrates that when reduced web units are used to ensure horizontal grout continuity stack pattern beams may be designed in the same manner as running bond beams.

KEYWORDS: *concrete masonry beam, stack and running bond construction, structural performance*

[1] PhD Candidate, Department of Civil and Environmental Engineering, University of Windsor, 401 Sunset Ave., Windsor, ON, Canada, zohreh@uwindsor.ca
[2] Professor, Department of Civil and Environmental Engineering, University of Windsor, 401 Sunset Ave., Windsor, ON, Canada, sdas@uwindsor.ca
[3] Masonry Research and Development Engineer, Canada Masonry Design Centre, 360 Superior Blvd., Mississauga, ON, Canada, Bbanting@canadamasonrycentre.com

INTRODUCTION

Loadbearing reinforced concrete masonry (RM) construction is traditionally built using a 50% running bond (RB) pattern (Figure 1a). In recent years, an increase in demand for stack pattern (SP) masonry has risen due to its aesthetic properties. This concept involves the stacking of the masonry units directly above each other such that all the head joints are aligned (Figure 1b). Since there has been no relevant research undertaken to evaluate the structural competency of SP masonry beams, CSA [1] recommends that masonry beams be built using the RB construction. Hence, the use of SP beams in Canada is restricted to decorative and nonloadbearing purposes only.

(a) Running Bond (b) Stack Pattern

Figure 1: Running Bond and Stack Pattern Construction

A major concern in the behaviour of SP masonry beams is the development of flexural cracks through the continuous vertical mortar joints. Crack location, width and pattern development in a masonry beam during loading is an indication of how it may perform at ultimate load. Essentially, the denser and wider the cracks develop during loading, the weaker the beam becomes. Many studies have been completed to evaluate, prevent or minimise the development of tensile and shear cracks in masonry and concrete beams. Some of the methods used to reduce excessive cracking in beams is the use of fiber reinforced polymers (FRP) [2], skin reinforcement [3], the use of intermediate steel [4] or even the use of bamboo as reinforcement [5].

For traditional RB beams, vertical cracks through head joints develop and grow until they are interrupted by an overlapping block. Since there is no available test data on SP beam specimens, only a presumption can be made regarding flexural cracks in these beams. The supposition is that since the vertical cracks through the mortar head joints of a SP beam are not interrupted by blocks in the preceding course, it leads to a larger deflection, causing the beam to fail at a lower load. This study was completed to verify if the supposition is valid.

EXPERIMENTAL PROGRAMS

The summary of material properties obtained from mortar, grout, and concrete block unit tests are shown in Table 1 [6-8].

Table 1: Material properties

Materials	Beam test-day values	
	Strength (MPa)	C.O.V. (%)
Block	18.2	2.2
Mortar	16.0	8.1
Grout	22.5	7.7
Reinforcement	Yield Stress = 450.0	5.9

PRISMS TESTS

The prism specimens were divided into 4 sets of 5 specimens. The test setup for the prisms is shown in Figure 2. Nominal dimensions of the block units were 400 mm long, 200 mm wide, and 200 mm deep. A compressive load was applied monotonically. First, 45 to 50 % of the failure load was applied while two 5 mm LDTs on each side of the prism acquired deflection measurements. Then the LDTs were removed and load was reapplied monotonically until failure occurred.

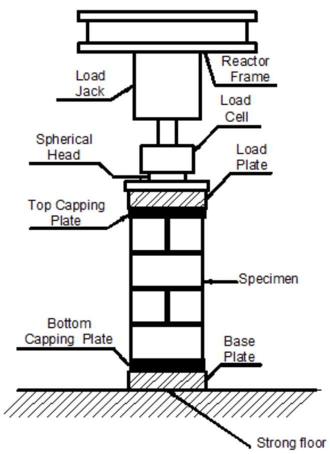

(a) Depiction of Test Setup

(b) Photograph of Test Setup

Figure 2: Prism Test Setup

Test matrix for prism specimens is shown in Table 2. Specimen, SN indicates that this prism specimen was built using SP construction (S) and the load was applied normal to bed joint (N). Specimen, RP was built using RB construction (R) and the load was applied parallel to bed joint (P). Failure in the prism specimens were either due to separation of the face shell from the grout or due to complete crushing of the grout.

As can be found in Table 2, the running bond prisms exhibited a slightly higher strength than stack pattern prisms. The differences are 10% and 22% for specimens loaded normal to bed joint and specimens loaded parallel to bed joint, respectively. It is not obvious why stack pattern prisms showed much lower strength when load was applied parallel to the bed joint. It is also worth noting that the χ-factor mentioned in the CSA S304 [1] is over conservative given that the strengths of SP and RP were actually greater than the strengths of SN and RN, respectively.

Table 2: Fully-Grouted Prism Specimen Results

Specimen Name	SN	RN	SP	RP
Specimen ID	1 to 5	1 to 5	1 to 5	1 to 5
C.O.V.	11.3%	14.7%	11.9%	7.58%
f'_m (MPa)	9.7	10.7	15.5	19.98
Prism Elevation	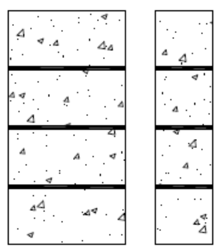	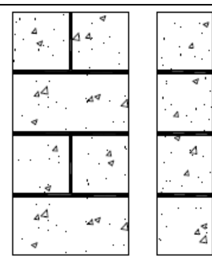	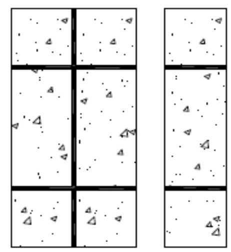	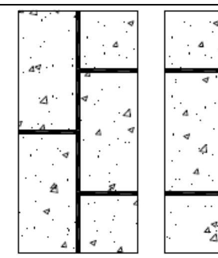

DIGITAL IMAGE CORRELATION

Digital Image Correlation (DIC) is a non-contact measurement technique that has been implemented in civil engineering applications recently. The main objective of using DIC was to determine the strain contour, the modulus of elasticity (E_m) of the prisms, and to monitor deformation and the crack growth in the beams. A commercially available software was used for collecting the images through cameras. DIC is a virtual alternative to instrumentation mounted directly on the specimen. The major advantage with the DIC technique is the flexibility to place virtual extensometers and strain gauges on the specimen. Since DIC works on the pixels, an unlimited number of strain gauges and extensometers can be considered. The number of the strain gauges (pixels) that was used in a four course prism specimen in this study is about 140,000.

Figure 3 shows the locations of the crack formations just before the failure occurred. It is worth noting that since the failure of prism specimens is violent and sudden, camera were removed before failure occurred. Figures 3a and 3b show the critical locations for strain concentrations in x and y directions. Figure 3c is a picture of the failed prism specimen and this figure confirms that the DIC was able to detect the location of failure which otherwise is impossible by other means.

Figure 4 shows load-deformation curve for normal to the bed joint prism (SN) under elastic loads. Figure 4a shows the load-deformation curve obtained from Linear Variable Displacement Transducer (LVDT) and Figure 4b shows the same load-deformation curve once the obvious errors in the measurements are removed. The LVDT used in this study has an accuracy of ±0.1%. In Figure 4b, the test data was the fitted with a linear curve with R^2 of 0.99.

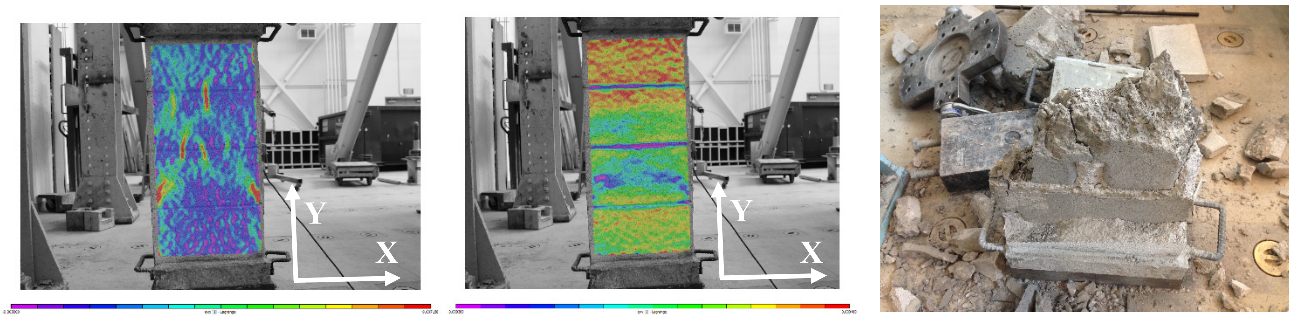

(a) e_{xx} **(b) e_{yy}** **(c) Failure**

Figure 3: Strain Contour in DIC and Failure

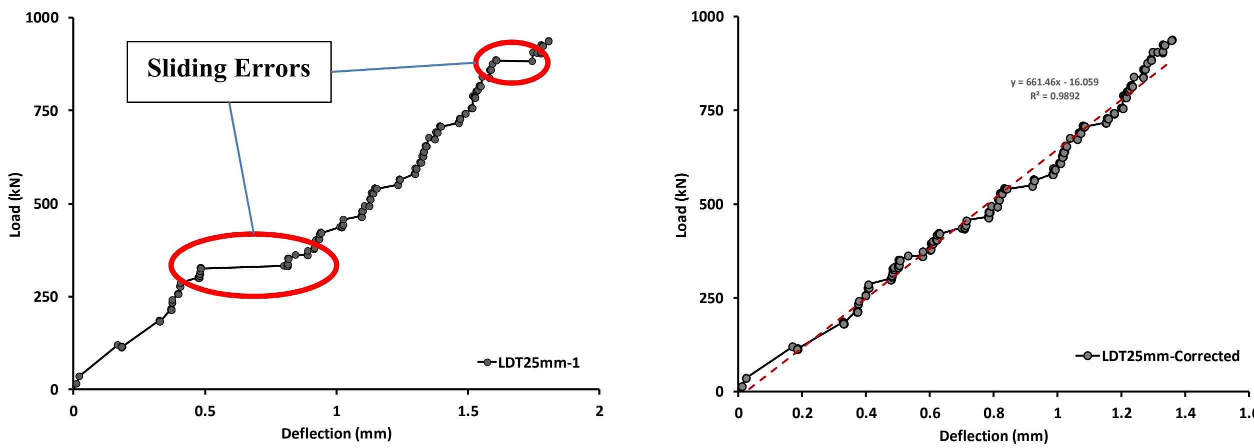

(a) Before Correction (b) After Correction

Figure 4: Typical Error in Elastic Displacement Data obtained by LVDT

Figure 5 shows the load-deformation curve obtained from the same prism specimen using DIC including inelastic deformation. This figure shows that the load-deformation curve is non-linear and this agrees with the previous study [9]. Hence, DIC is able to acquire the non-linearity in the load-deformation behaviour and thus, in the stress-strain behaviour as well. Two different curve fittings are also shown in Figure 5. The first one with a linear fit which has R^2 of 0.77. However, the R^2 value improves to 0.93 if the test data is fitted with a second order polynomial. Subsequently, best fitted load-deformation curses obtained from LVDT and DIC were used to determine the modulus of elasticity of masonry (E_m) and the values are 12 GPa and 8.5 GPa, respectively. The value of E_m obtained from the DIC data correlates better with the recommendation of the Canadian standard, CSA S304 [1].

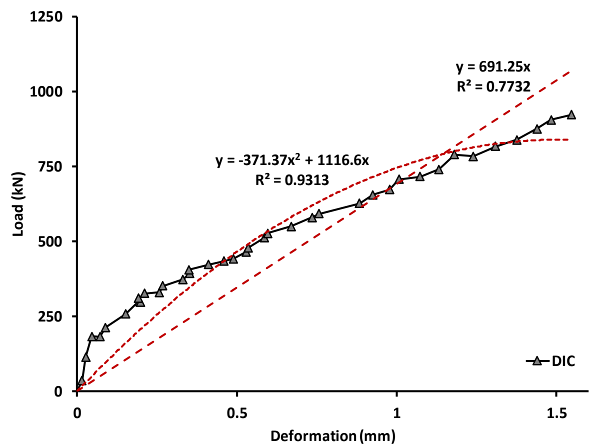

Figure 5: Inelastic Load-Deflection Behaviour of Masonry Prism obtained from DIC

BEAM TESTS

The study included testing of eight full-scale masonry beam specimens (Table 3). Each beam was 4.8 m long and 200 mm wide and the clear span of each beam specimen was 4.2 m. The effective depth of the longitudinal steel rebars was 300 mm and 500 mm for two-course and three-course height beam specimens, respectively. The beam specimens had pin-roller simply supported boundary condition. The beam specimens were built of standard knock-out units except at the bottom course where lintel blocks were used to facilitate the placement of main flexural rebar (Figure 6).

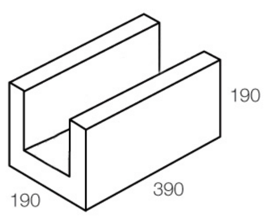

(a) Lintel Blocks

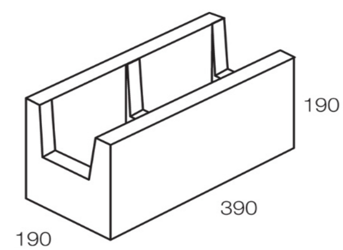

(a) Knock-out Block

Figure 6: Lintel and Knock-out blocks in Masonry Construction

Nominal dimensions of the block units were 400 mm long, 200 mm wide, and 200 mm deep. The beams were designed as under-reinforced beams according to the CSA S304 [1]. Type S mortar and fine grout was used in accordance with Canadian standard CSA-A179 [4]. Specimen names in Table 3 are self-explanatory. For example, beam specimen RN2 indicates that this beam was built using running bond pattern (R), it had no shear reinforcement (N), and it was two-course high (2). Hence, beam specimen SY3 was a three-course high (3) beam and built with stack pattern construction (S), and it had shear reinforcement (Y). The load was applied using a steel spreader beam to create a constant moment zone length of 700 mm. The test set-up is shown in Figure 7. As can be found in Figure 7, three LVDTs were mounted at every third span of the beam to capture the deformation profile and mid-span deflection. Loadcell was used to acquire the load data. Load was gradually applied to the beams using a displacement control method and the loading was continued until a clear failure mode was visible in the beam.

BEAM TEST RESULTS

The load-deformation curves obtained from this study (Figure 8) show that no reduction in shear or flexural capacity is apparent when beams are built using SP construction. This finding contradicts the current general belief and the recommendation of the Canadian standard [1] for ultimate strength conditions. Hence, this study suggests that though the cracks form quicker and longer in SP beams, these cracks do not affect the strength of these beams. Hence, based on the results obtained from this study, it can be concluded that irrespective of construction patterns (SP or RB) these cracks are superficial, and do not affect the beam capacity until they are deep enough to split the grout. The tests on beam specimens which were reinforced with stirrups were stopped as the crack widths became larger (8 to 10 mm) because when the crack width grew beyond 10 mm, the beam was well into the plastic deformation. The cracks are located in the vertical mortar joints at centre span which was subjected to the maximum moment. The presence of stirrups reduced or eliminated the crack height of the beam. Each test was discontinued for safety reasons when the crack width reached about 10 mm. It can be concluded that adopting reduced web units does not measurably produce any significant reduction to ultimate strength of stack pattern beams.

Table 3: Beam Specimen Matrix

Beam Type	Beam Specimens				Bond Pattern	Stirrup (Total)	Bottom Rebar	Top Rebar
	No.	Name	L mm	H mm				
2-course	1	RN2	4800	390	Running	None	2 - 10M	None
	2	RY2				10M @ 200 (24)	2 - 10M	1 - 10M
	3	SN2			Stack	None	2 - 10M	None
	4	SY2				10M @ 200 (24)	2 - 10M	1 - 10M
3 - course	5	RN3		590	Running	None	2 - 10M	None
	6	RY3				10M @ 200 (24)	2 - 10M	1 - 10M
	7	SN3			Stack	None	2 - 10M	None
	8	SY3				10M @ 200 (24)	2 - 10M	1 - 10M

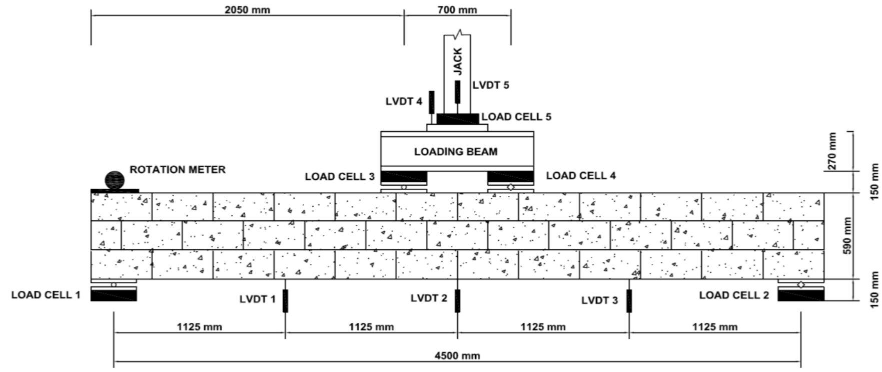

Figure 7: Beam Test Setup

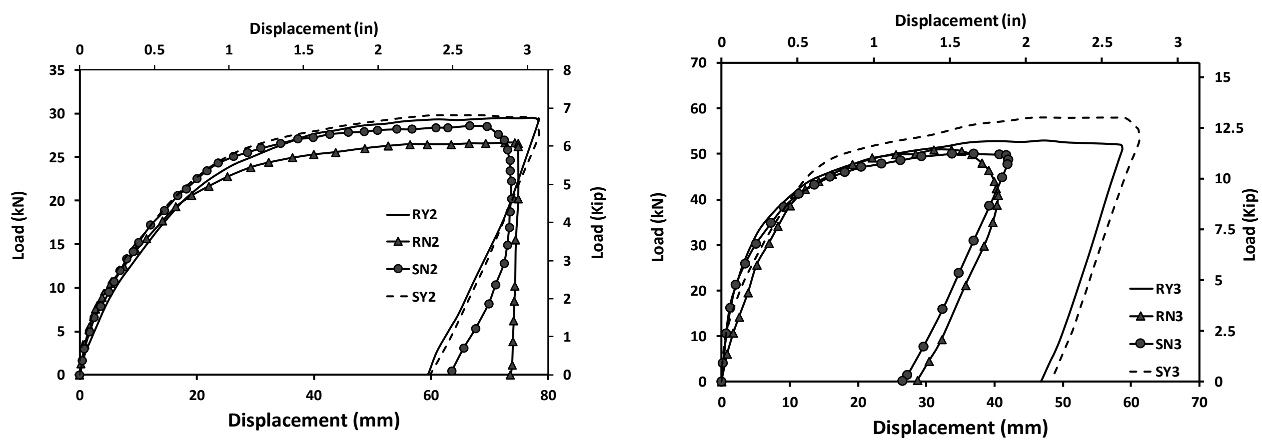

(a): Two-Course Beams **(b): Three-Course Beams**

Figure 8: Load-Deflection Curves

Serviceability and Crack Control

At the crack control service load, defined as the 60% of the yield strength of the main tension reinforcement in accordance with CSA S304 [1], vertical cracking in the mortar joints for the SP beams were more prominent than the RB beams. For both RB and SP beam types, at the crack control service load state, cracks were longer and became denser as the slenderness of the beam increased. However, crack widths at the crack control service load were all much less than 1 mm and they were visible with the use of a high definition camera only. Figure 9 shows the use of DIC to determine to crack width in beam specimen, RN3. The vertical axis in Figure 9 shows the displacement of the beam in X-direction and horizontal axis is the number of pixels. As discussed earlier, DIC works based on the pixels. The horizontal displacement of each pixel along any reference line (such as one shown by a thick black line AB) are measured by DIC. Thus, DIC does not measure the crack width directly. Instead, the crack width can be determined indirectly by calculating the difference in two values of the displacements (U in Figure 9); one just at the left of the crack and the second value just at the right of the crack.

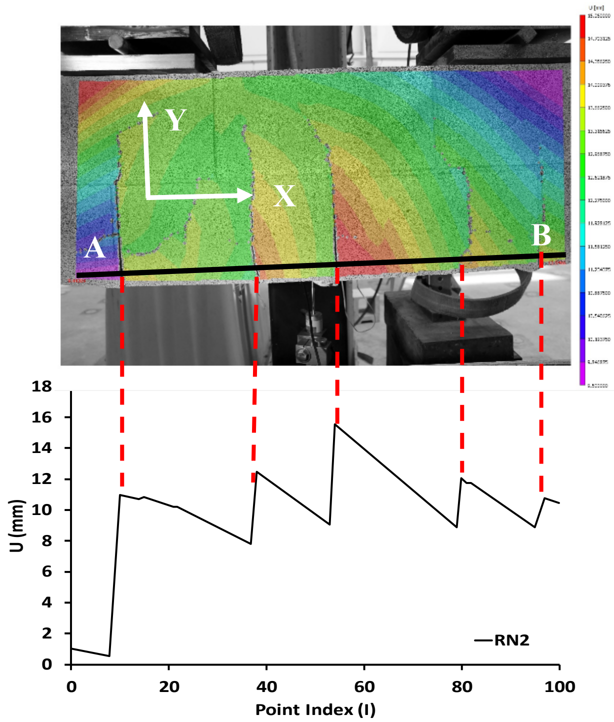

Figure 9: Calculation of Crack Width by Using DIC Technique for RN3

Table 4 is a summary for each beam specimen showing the vertical displacement, strain, load and crack patterns at the crack control service load (SL) and ultimate load (UL). Also, specimens being directly compared have been grouped together with a thicker line. For some cases, the strain gauges broke before the ultimate load capacity reached. In that case, the maximum strain recorded before the strain gauge stopped working is displayed with an asterisk beside it. Similarly, if no cracks are present at the service load, NV (not visible) is indicated.

CONCLUSIONS

The load deformation curves obtained from the beam tests, showed that the initial stiffness as well as ultimate strength for stack pattern and running bond masonry beams are essentially identical. This is not expected when referring the presumptions made by CSA S304 (Clause 11.1.3). Rather, the use of concrete masonry units with webs reduced to approximately 50% the unit height were sufficient in providing enough grout continuity in SP beams to overcome any effects of the vertically aligned head joints. As the load on the beam increased, crack depths began to reach the grout. Once the crack depth reached the grout the patterns for the two beams (SP and RB beams) began to converge to similar patterns regarding spacing, height, and width.

Further analysis revealed that the presence of stirrups has increased the spacing and decreased the height of the cracks present at the crack control service load. In some cases, cracks failed to develop at all. Therefore, it can also be concluded that span-to-depth ratio and the presence of shear stirrups play a much more significant role in mitigating serviceability cracking than the bonding pattern of the units.

Table 4: Summary of Beam Results

Name	Pattern	Load Stage	Moment (kN·m)	Deflection (mm)	Strain (%)	Crack Width (mm)	Crack Height (mm)	Crack Spacing (mm)	Failure Mode
RN2	RB	SL	22.8	8	0.12	<1	200	400	Flexural
		UL	47.5	73	2.00	9	375	133	
SN2	SP	SL	22.8	8	0.12	<1	250	400	Flexural
		UL	57.0	70	*1.00	9	400	133	
RY2	RB	SL	22.8	11	0.12	NV	NV	NV	Flexural
		UL	57.0	78	4.00	5.5	350	200	
SY2	SP	SL	22.8	9	0.12	<1	190	400	Flexural
		UL	57.0	78	3.00	7.5	365	200	
RN3	RB	SL	47.5	6	0.12	<1	200	NV	Shear
		UL	95	40	1.80	6	400	400	
SN3	SP	SL	45.6	4	0.12	<1	200	NV	Shear
		UL	96.9	42	2.10	8	500	200	
RY3	RB	SL	47.5	3	0.12	NV	NV	NV	Flexural
		UL	100.5	58.4	4.00	8	575	150	
SY3	SP	SL	45.6	5	0.12	NV	NV	NV	Flexural
		UL	112.5	60.6	4.5	6	550	200	

Note: SL = Service Load, UL = Maximum Load, NV = Not Visible, * indicates maximum strain gauge reading before it broke

ACKNOWLEDGEMENTS

This work was completed with the financial assistance from the Natural Sciences and Engineering Research Council (NSERC) and Canada Masonry Design Centre (CMDC). The authors sincerely thank Con-tact Masonry Ltd. located in Windsor for their support and help. Special thanks to Kyle Gerard, Lucian Pop, Matthew St. Louis, and many graduate students for their help.

REFERENCES

[1] CSA: Canadian Standards Association. (2014). “S304-14 Design of Masonry Structures,” CSA Standard, CSA, Mississauga, Ontario, Canada, 180 pp.

[2] Lee, C., Kim, J. and Heo, S. (2010). “Experimental Observation on the Effectiveness of Fiber Sheet Strip Stirrups in Concrete Beams,” Journal of Composites for Construction, 14(5), pp.487-497.

[3] Ring, T., Das, S. and Stubbs, D. (2012). Compressive Strength of Concrete Masonry Beams. Structural Journal, 109(3), 2012, pp.369-376.

[4] Frosch, R. (2002). “Modeling and Control of Side Face Beam Cracking,” ACI Structural Journal, pp. 376-385.

[5] Moroz, J., Lissel, S., & Hagel, M. (2014). “Performance of bamboo reinforced concrete masonry shear walls,” Construction and Building Materials, 61, pp. 125-137.

[6] CSA: Canadian Standards Association. (2014). “A165 SERIES-14: Concrete Blcok Masonry Units,” CSA Standard, CSA, Mississauga, Ontario, Canada, 54 pp.

[7] CSA: Canadian Standards Association. (2014). “A179-14: Mortar and Grout for Unit Masonry,” CSA Standard, CSA, Mississauga, Ontario, Canada, 74 pp.
[8] ASTM C1019-14. (2013). “Standard Test Method for Sampling and Testing Grout,” ASTM Int., pp. 3–6.
[9] Hamid, A. A. (1997). “Material Model for Concrete and Clay Masonry”, Journal of the Masonry Society, Vol. 15, No. 1, pp. 21-26.
[10] ACI Committee 318. (1999). “Building code requirements for structural concrete: (ACI 318-99); and commentary (ACI 318R-99),”. Farmington Hills, Mich: American Concrete Institute